UMTS Capacity and Throughput Maximization for Different Spreading Factors

Robert Akl and Son Nguyen
Dept. of Computer Science and Engineering, University of North Texas
Denton, Texas, 76207
Email: {rakl, stn}@cse.unt.edu

Abstract— **An analytical model for calculating capacity in multi-cell UMTS networks is presented. Capacity is maximized for different spreading factors and for perfect and imperfect power control. We also design and implement a local call admission control (CAC) algorithm which allows for the simulation of network throughput for different spreading factors and various mobility scenarios. The design of the CAC algorithm uses global information; it incorporates the call arrival rates and the user mobilities across the network and guarantees the users' quality of service as well as pre-specified blocking probabilities. On the other hand, its implementation in each cell uses local information; it only requires the number of calls currently active in that cell. The capacity and network throughput were determined for signal-to-interference threshold from 5 dB to 10 dB and spreading factor values of 256, 64, 16, and 4.**

Index Terms— **WCDMA, Call Admission Control, Mobility, Network Throughput, Optimization.**

I. Introduction

3G cellular systems are identified as International Mobile Telecommunications-2000 under International Telecommunication Union and as Universal Mobile Telecommunications Systems (UMTS) by European Telecommunications Standards Institute. Besides voice capability in 2G, the new 3G systems are required to have additional support on a variety of data-rate services using multiple access techniques. Code Division Multiple Access (CDMA) is the fastest-growing digital wireless technology since its first commercialization in 1994. The major markets for CDMA are North America, Latin America, and Asia (particularly Japan and Korea). In total, CDMA has been adopted by more than 100 operators across 76 countries around the globe [1].

Since the first comparisons of multiple access schemes for UMTS [2], which found that Wideband CDMA (WCDMA) was well suited for supporting variable bit rate services, several research on WCDMA capacity has been considered. In [3], the authors present a method to calculate the WCDMA reverse link Erlang capacity based on the Lost Call Held (LCH) model as described in [4]. This algorithm calculates the occupancy distribution and capacity of UMTS/WCDMA systems based on a system outage condition. The authors derive a closed form expression of Erlang capacity for a single type of traffic loading and compare analytical results with simulations results.

The same LCH model was also used in [5] to calculate the forward link capacity of UMTS/WCDMA systems based on the system outage condition. In the forward link, because many users share the base station (BS) transmission power, the capacity is calculated at the BS. The transmission power from the BS is provided to each user based on each user's relative need. The access in the calculation of forward link capacity is one-to-many rather than many-to-one as in the reverse link. The authors provide capacity calculation results and performance evaluation through simulation.

An alternate approach, where mobile stations (MSs) are synchronized on the uplink, i.e., signals transmitted from different MSs are time aligned at the BS, has been considered. Synchronous WCDMA looks at time synchronization for signal transmission between the BS and MS to improve network capacity. The performance of an uplink-synchronous WCDMA is analyzed in [6]. Scrambling codes are unique for each cell. MSs in the same cell share the same scrambling code, while different orthogonal channelization codes are derived from the set of Walsh codes. In [6], the potential capacity gain is about 35.8% in a multi-cell scenario with infinite number of channelization codes per cell and no soft handoff capability between MSs and BSs. However, the capacity gain in a more realistic scenario is reduced to 9.6% where soft handoff is enabled. The goal of this uplink-synchronous method in WCDMA is to reduce intra-cell interference. But the implementation is fairly complex while the potential capacity gain is not very high.

Our contributions are two-fold. First, we calculate the maximum reverse link capacity in UMTS/WCDMA systems for both perfect and imperfect power control with a given set of quality of service requirements and for different spreading factors. Second, we also design, analyze, and simulate a local CAC algorithm for UMTS networks by formulating an optimization problem that maximizes the network throughput for different spreading factors using signal-to-interference constraints as lower bounds. The solution to this problem is the maximum number of calls that can be admitted in each cell. The design is optimized for the entire network, and the im-

Based on Capacity Allocation in Multi-cell UMTS Networks for Different Spreading Factors with Perfect and Imperfect Power Control, by R. Akl and S. Nguyen, which appeared in the Proceedings of IEEE CCNC 2006: Consumer Communications and Networking Conference, vol. 2, pp. 928-932, January 2006.

plementation is simple and considers only a single cell for admitting a call. Numerical results are presented for signal-to-interference thresholds from 5 dB to 10 dB and spreading factor values of 256, 64, 16, and 4.

The remainder of this paper is organized as follows. The user and interference models are presented in Section II. In Section III, we analyze capacity for perfect and imperfect power control. In Section IV, we describe our call admission control algorithm. Network throughput is determined in Section V. Spreading factors are discussed in Section VI. Numerical results are presented in Section VII, and finally Section VIII concludes the paper.

II. User and Interference Model

This study assumes that each user is always communicating and is power controlled by the BS that has the highest received power at the user. Let $r_i(x,y)$ and $r_j(x,y)$ be the distance from a user to BS i and BS j, respectively. This user is power controlled by BS j in the cell or region C_j with area A_j, which BS j services. This study assumes that both large scale path loss and shadow fading are compensated by the perfect power control mechanism. Let $I_{ji,g}$ be the average inter-cell interference that all users $n_{j,g}$ using services g with activity factor v_g and received signal S_g at BS j impose on BS i. Modifying the average inter-cell interference given by [7], it becomes

$$I_{ji}^{(g)} = S_g v_g n_{j,g} \frac{e^{(\beta\sigma_s)^2}}{A_j} \int\int_{C_j} \frac{r_j^m(x,y)}{r_i^m(x,y)} w(x,y)\, dA(x,y), \tag{1}$$

where $\beta = \ln(10)/10$, σ_s is the standard deviation of the attenuation for the shadow fading, m is the path loss exponent, and $w(x,y)$ is the user distribution density at (x,y). Let $\kappa_{ji,g}$ be the per-user (with service g) relative inter-cell interference factor from cell j to BS i,

$$\kappa_{ji,g} = \frac{e^{(\beta\sigma_s)^2}}{A_j} \int\int_{C_j} \frac{r_j^m(x,y)}{r_i^m(x,y)}\, w(x,y)\, dA(x,y). \tag{2}$$

The inter-cell interference density I_{ji}^{inter} from cell j to BS i from all services G becomes

$$I_{ji}^{inter} = \frac{1}{W} \sum_{g=1}^{G} I_{ji}^{(g)}, \tag{3}$$

where W is the bandwidth of the system. Eq. (3) can be rewritten as

$$I_{ji}^{inter} = \frac{1}{W} \sum_{g=1}^{G} S_g v_g\ n_{j,g}\ \kappa_{ji,g}. \tag{4}$$

Thus, the total inter-cell interference density I_i^{inter} from all other cells to BS i is

$$I_i^{inter} = \frac{1}{W} \sum_{j=1,j\neq i}^{M} \sum_{g=1}^{G} S_g v_g\ n_{j,g}\ \kappa_{ji,g}, \tag{5}$$

where M is the total number of cells in the network.

If the user distribution density can be approximated, then, $\kappa_{ji,g}$ needs to be calculated only once. The user distribution is modeled with a 2-dimensional Gaussian function as follows [8]

$$w(x,y) = \frac{\eta}{2\pi\sigma_1\sigma_2} e^{-\frac{1}{2}(\frac{x-\mu_1}{\sigma_1})^2} e^{-\frac{1}{2}(\frac{y-\mu_2}{\sigma_2})^2}, \tag{6}$$

where η is a user density normalizing parameter.

By specifying the means μ_1 and μ_2 and the standard deviations σ_1 and σ_2 of the distribution for every cell, an approximation can be found for a wide range of user distributions ranging from uniform to hot-spot clusters. These results are compared with simulations to determine the value of η experimentally.

III. UMTS Capacity

A. Capacity with Perfect Power Control

In WCDMA, with perfect power control (PPC) between BSs and MSs, the energy per bit to total interference density at BS i for a service g is given by [9]

$$\left(\frac{E_b}{I_0}\right)_{i,g} = \frac{\frac{S_g}{R_g}}{N_0\ +\ I_i^{inter}\ +\ I_i^{own}\ -\ S_g v_g}, \tag{7}$$

where N_0 is the thermal noise density, and R_g is the bit rate for service g. I_i^{inter} was calculated in section II. I_i^{own} is the total intra-cell interference density caused by all users in cell i. Thus I_i^{own} is given by

$$I_i^{own} = \frac{1}{W} \sum_{g=1}^{G} S_g v_g n_{i,g}. \tag{8}$$

Let τ_g be the minimum signal-to-noise ratio, which must received at a BS to decode the signal of a user with service g, and S_g^* be the maximum signal power, which the user can transmit. Substituting (5) and (8) into (7), we have for every cell i in the UMTS network, the number of users $n_{i,g}$ in BS i for a given service g needs to meet the following inequality constraints

$$\tau_g \leq \frac{\frac{S_g^*}{R_g}}{N_0 + \frac{S_g^*}{W}\left[\sum_{g=1}^{G} n_{i,g}v_g + \sum_{j=1,j\neq i}^{M}\sum_{g=1}^{G} n_{j,g}v_g\kappa_{ji,g} - v_g\right]}, \quad \text{for } i=1,...,M. \tag{9}$$

After rearranging terms, (9) can be rewritten as

$$\sum_{g=1}^{G} n_{i,g}v_g + \sum_{j=1,j\neq i}^{M}\sum_{g=1}^{G} n_{j,g}v_g\kappa_{ji,g} - v_g \leq c_{eff}^{(g)}, \quad \text{for } i=1,...,M, \tag{10}$$

where

$$c_{eff}^{(g)} = \frac{W}{R_g}\left[\frac{1}{\tau_g} - \frac{R_g}{S_g^*/N_0}\right]. \tag{11}$$

The maximized capacity in a UMTS network is defined as the maximum number of simultaneous users $(n_{1,g}, n_{2,g}, ..., n_{M,g})$ for all services $g = 1, ..., G$ that satisfy (10).

B. Capacity with Imperfect Power Control

The calculation of UMTS network capacity, which was formulated in section III-A, assumes perfect power control between the BSs and MSs. However, transmitted signals between BSs and MSs are subject to multi-path propagation conditions, which make the received $\left(\frac{E_b}{I_o}\right)_{i,g}$ signals vary according to a log-normal distribution with a standard deviation on the order of 1.5 to 2.5 dB [4]. Thus, in the imperfect power control (IPC) case, the constant value of $(E_b)_{i,g}$ in each cell i for every user with service g needs to be replaced by the variable $(E_b)_{i,g} \stackrel{\triangle}{=} \epsilon_{i,g}(E_b)_{o,g}$, which is log-normally distributed. We define

$$x_{i,g} = 10\log_{10}\left(\frac{\epsilon_{i,g}(E_b)_{o,g}}{I_0}\right), \tag{12}$$

to be a normally distributed random variable with mean m_c and standard deviation σ_c.

According to [4], by evaluating the nth moment of $\epsilon_{i,g}$ using the fact that $x_{i,g}$ is Gaussian with mean m_c and standard deviation σ_c, then taking the expected value, we have

$$E\left[\frac{(E_b)_{o,g}}{I_0}\epsilon_{i,g}\right] = \frac{(E_b)_{i,g}}{I_0}\, e^{\frac{(\beta\sigma_c)^2}{2}}. \tag{13}$$

As a result of (13), $c^{(g)}_{eff\_IPC}$ becomes $c^{(g)}_{eff}$ / $e^{\frac{(\beta\sigma_c)^2}{2}}$.

IV. UMTS Call Admission Control

A. Feasible States

Recall from section III-A that the number of calls in every cell must satisfy (10). A set of calls $\mathbf{n}$ satisfying (10) is said to be in feasible call configuration or a feasible state, which meet the $\frac{E_b}{I_0}$ constraint.

Denote by Ω the set of feasible states. Define the set of blocking states for service g in cell i as

$$\mathcal{B}_{i,g} = \left\{ \mathbf{n} \in \Omega : \begin{bmatrix} n_{1,1} & \dots & n_{1,G} \\ \dots & \dots & \dots \\ n_{M,1} & \dots & n_{M,G} \end{bmatrix} \notin \Omega \right\}. \tag{14}$$

If a new connection or a handoff connection with the service g arrives to cell i, it is blocked when the current state of the network, $\mathbf{n}$, is in $\mathcal{B}_{i,g}$.

B. Mobility Model

There are several mobility models that have been discussed in the literature [10]–[12]. These models have ranged from general dwell times for calls to ones that have hyper-exponential and sub-exponential distributions. For the CAC problem that we are investigating here, however, such assumptions makes the problem mathematically intractable. The mobility model that we use is presented in [13] where a call stops occupying a cell either because user mobility has forced the call to be handed off to another cell, or because the call is completed.

The call arrival process with service g to cell i is assumed to be a Poisson process with rate $\lambda_{i,g}$ independent of other call arrival processes. The call dwell time is a random variable with exponential distribution having mean $1/\mu$, and it is independent of earlier arrival times, call durations and elapsed times of other users. At the end of a dwell time a call may stay in the same cell, attempt a handoff to an adjacent cell, or leave the network. Define $q_{ii,g}$ as the probability that a call with service g in progress in cell i remains in cell i after completing its dwell time. In this case, a new dwell time that is independent of the previous dwell time begins immediately. Let $q_{ij,g}$ be the probability that a call with service g in progress in cell i after completing its dwell time goes to cell j. If cells i and j are not adjacent, then $q_{ij,g} = 0$. We denote by $q_{i,g}$ the probability that a call with service g in progress in cell i departs from the network.

This mobility model is attractive because we can easily define different mobility scenarios by varying the values of these probability parameters [13]. For example, if $q_{i,g}$ is constant for all i and g, then the average dwell time of a call of the same service in the network will be constant regardless of where the call originates and what the values of $q_{ii,g}$ and $q_{ij,g}$ are. Thus, by varying $q_{ii,g}$'s and $q_{ij,g}$'s for a service g, we can obtain low and high mobility scenarios and compare the effect of mobility on network attributes (e.g., throughput).

We assume that the occupancy of the cells evolves according to a birth-death process, where the total arrival rate or offered traffic for service g to cell i is $\rho_{i,g}$, and the departure rate from cell i when the network is in state $\mathbf{n}$ is $n_{i,g}\mu_{i,g} = n_{i,g}\mu(1 - q_{ii,g})$. Let ρ be the matrix of offered traffic of service g to the cells, μ the matrix of departure rates, and let $p(\rho, \mu, \mathbf{n})$ be the stationary probability that the network is in state $\mathbf{n}$. The new call blocking probability for service g in cell i, $B_{i,g}$, is given by

$$B_{i,g} = \sum_{\mathbf{n}\in\mathcal{B}_{i,g}} p(\rho, \mu, \mathbf{n}). \tag{15}$$

This is also the blocking probability of handoff calls due to the fact that handoff calls and new calls are treated in the same way by the network.

Let $\mathcal{A}_i$ be the set of cells adjacent to cell i. Let $\nu_{ji,g}$ be the handoff rate out of cell j offered to cell i for service g. $\nu_{ji,g}$ is the sum of the proportion of new calls of service g accepted in cell j that go to cell i and the proportion of handoff calls with service g accepted from cells adjacent to cell j that go to cell i. Thus

$$\nu_{ji,g} = \lambda_{j,g}(1 - B_{j,g})q_{ji,g} + (1 - B_{j,g})q_{ji,g} \sum_{x\in\mathcal{A}_j} \nu_{xj,g}. \tag{16}$$

Equation (16) can be rewritten as

$$\nu_{ji,g} = \nu(B_{j,g}, \rho_{j,g}, q_{ji,g}) = (1 - B_{j,g})q_{ji,g}\rho_{j,g}, \tag{17}$$

where $\rho_{j,g}$, the total offered traffic to cell j for service g, is given by

$$\rho_{j,g} = \rho(\mathbf{v}, \lambda_{j,g}, \mathcal{A}_j) = \lambda_{j,g} + \sum_{x\in\mathcal{A}_j} \nu_{xj,g}, \tag{18}$$

and where **v** denotes the matrix whose components are the handoff rates ν_{ij} for $i, j = 1, ...M$.

The total offered traffic can be obtained from a fixed point model [14], which describes the offered traffic as a function of the handoff rates and new call arrival rates, the handoff rates as a function of the blocking probabilities and the offered traffic, and the blocking probabilities as a function of the offered traffic. For a given set of arrival rates, we use an iterative method to solve the fixed point equations. We define an initial value for the handoff rates. We calculate the offered traffic by adding the given values of the arrival rates to the handoff rates. The blocking probabilities are now calculated using the offered traffic. We then calculate the new values of the handoff rates and repeat. This approach has been extensively utilized in the literature to obtain solutions of fixed point problems [15]–[20]. The questions of existence and uniqueness of the solution and whether the iterative approach in fact converges to the solution (if a unique solution exists) are generally difficult to answer due to the complexity of the equations involved. Kelly has shown that for fixed alternate routing the solution to the fixed point problem is in fact not unique [21]; in all the numerical examples we solved, the iterative approach converged to a unique solution.

C. Admissible States

A CAC algorithm can be constructed as follows. A call arriving to cell i with service g is accepted if and only if the new state is a *feasible* state. Clearly this CAC algorithm requires global state, i.e., the number of calls in progress in all the cells of the network. Furthermore, to compute the blocking probabilities, the probability of each state in the feasible region needs to be calculated. Since the cardinality of Ω is $O({c_{eff}}^{MG})$, the calculation of the blocking probabilities has a computational complexity that is exponential in the number of cells combined with number of available services.

In order to simplify the CAC algorithm, we consider only those CAC algorithms which utilize local state, i.e., the number of calls in progress in the current cell. To this end we define a state **n** to be *admissible* if

$$n_{i,g} \leq \ N_{i,g} \quad \text{for} \quad i = 1, ..., M \text{ and } g = 1, ..., G, \quad (19)$$

where $N_{i,g}$ is a parameter which denotes the maximum number of calls with service g allowed to be admitted in cell i. Clearly the set of admissible states denoted Ω' is a subset of the set of feasible states Ω. The blocking probability for cell i with service g is then given by

$$B_{i,g} = B(A_{i,g}, N_{i,g}) = \frac{A_{i,g}^{N_{i,g}}/N_{i,g}!}{\sum_{k=0}^{N_{i,g}} A_{i,g}^{k}/k!}, \quad (20)$$

where $A_i = \rho_{i,g}/\mu_{i,g} = \rho_{i,g}/\mu(1 - q_{ii,g})$ is the Erlang traffic in cell i with service g. We note that the complexity to calculate the blocking probabilities in (20) is $O(MG)$, and the bit error rate requirement is guaranteed since $\Omega' \subset \Omega$.

Once the maximum number of calls with different service that are allowed to be admitted in each cell, **N**, is calculated (this is done offline and described in the next section), the CAC algorithm for cell i for service g will simply compare the number of calls with service g currently active in cell i to $N_{i,g}$ in order to accept or reject a new arriving call. Thus our CAC algorithm is implemented with a computational complexity that is $O(1)$.

V. Network Throughput

The throughput of cell i consists of two components: the new calls that are accepted in cell i minus the forced termination due to handoff failure of the handoff calls into cell i for all services g. Hence the total throughput, T, of the network is

$$T(\mathbf{B}, \rho, \lambda) \quad = \quad \sum_{i=1}^{M} \sum_{g=1}^{G} \{\lambda_{i,g} - B_{i,g}\rho_{i,g}\}, \quad (21)$$

where $\mathbf{B}$ is the vector of blocking probabilities and λ is the matrix of call arrival rates.

A. Calculation of N

We formulate a constrained optimization problem in order to maximize the throughput subject to upper bounds on the blocking probabilities and a lower bound on the signal-to-interference constraints in (10). The goal is to optimize the utilization of network resources and provide consistent GoS while at the same time maintaining the QoS, β_g, for all the users for different services g. In this optimization problem the arrival rates are given and the maximum number of calls that can be admitted in all the cells are the independent variables. This is given in the following

$$\begin{aligned} \max_{\mathbf{N}} \quad & T(\mathbf{B}, \rho, \lambda), \\ \text{subject to} \quad & B(A_{i,g}, N_{i,g}) \leq \beta_g, \\ & \sum_{g=1}^{G} N_{i,g} v_g + \sum_{j=1, j\neq i}^{M} \sum_{g=1}^{G} N_{j,g} v_g \kappa_{ji,g} \\ & \qquad - v_g \leq c_{eff}^{(g)}, \\ & \text{for} \quad i = 1, ..., M. \end{aligned} \quad (22)$$

The optimization problem in (22) is solved offline to obtain the values of **N**.

B. Maximization of Throughput

A second optimization problem can be formulated in which the arrival rates and the maximum number of calls that can be admitted in all the cells are the independent

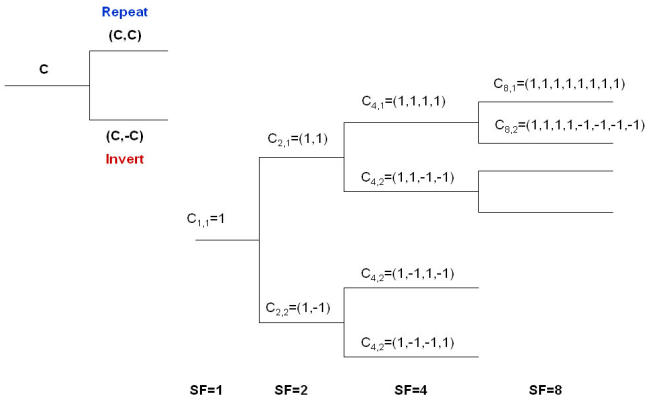

Fig. 1. Generation of OVSF codes for different Spreading Factors.

variables and the objective function is the throughput. This is given in the following

$$\begin{aligned} \max_{\lambda,\ \mathbf{N}} \quad & T(\mathbf{B}, \rho, \lambda), \\ \text{subject to} \quad & B(A_{i,g}, N_{i,g}) \leq \beta_g, \\ & \sum_{g=1}^{G} N_{i,g} v_g + \sum_{j=1, j\neq i}^{M} \sum_{g=1}^{G} N_{j,g} v_g \kappa_{ji,g} \\ & \qquad - v_g \leq c_{eff}^{(g)}, \\ & \text{for} \quad i = 1, ..., M. \end{aligned} \tag{23}$$

The optimized objective function of (23) provides an upper bound on the total throughput that the network can carry. This is the *network capacity* for the given GoS and QoS.

VI. Spreading Factor

Communication from a single source is separated by channelization codes, i.e., the dedicated physical channel in the uplink and the downlink connections within one sector from one MS. The Orthogonal Variable Spreading Factor (OVSF) codes, which were originally introduced in [22], were used to be channelization codes for UMTS.

The use of OVSF codes allows the orthogonality and spreading factor (SF) to be changed between different spreading codes of different lengths. Fig. 1 depicts the generation of different OVSF codes for different SF values.

The data signal after spreading is then scrambled with a scrambling codes to separate MSs and BSs from each other. Scrambling is used on top of spreading, thus it only makes the signals from different sources distinguishable from each other. Fig. 2 depicts the relationship between the spreading and scrambling process. Table I describes the different functionality of the channelization and the scrambling codes.

The typical required data rate or Dedicated Traffic Channel (DTCH) for a voice user is 12.2 Kbps. However, the Dedicated Physical Data Channel (DPDCH), which is the actual transmitted data rate, is dramatically increased due to the incorporated Dedicated Control Channel (DCCH) information, and the processes of Channel

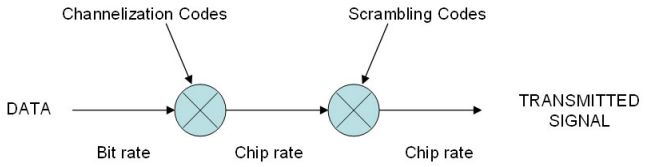

Fig. 2. Relationship between spreading and scrambling.

TABLE I
Functionality of the Channelization and Scrambling Codes.

	Channelization code	Scrambling code
Usage	Uplink: Separation of physical data (DPDCH) and control channels (DPCCH) from same MS Downlink: Separation of downlink connections to different MSs within one cell.	Uplink: Separation of MSs Downlink: Separation of sectors (cells)
Length	Uplink: 4-256 chips same as SF Downlink 4-512 chips same as SF	Uplink: 10 ms = 38400 chips Downlink: 10 ms = 38400 chips
Number of codes	Number of codes under one scrambling code = spreading factor	Uplink: Several millions Downlink: 512
Code family	Orthogonal Variable Spreading Factor	Long 10 ms code: Gold Code Short code: Extended S(2) code family
Spreading	Yes, increases transmission bandwidth	No, does not affect transmission bandwidth

Coding, Rate Matching, and Radio Frame Alignment. Fig. 3 depicts the process of creating the actual transmitted signal for a voice user. Fig. 4 shows the DPDCH data rate requirement for 64 Kbps data user. Table II shows the approximation of the maximum user data rate with $\frac{1}{2}$ rate coding for different values of DPDCH.

VII. Numerical Results

The results shown are for a twenty-seven cell network topology used in [23], [24]. The COST-231 propagation model with a carrier frequency of 1800 MHz, average base station height of 30 meters and average mobile height

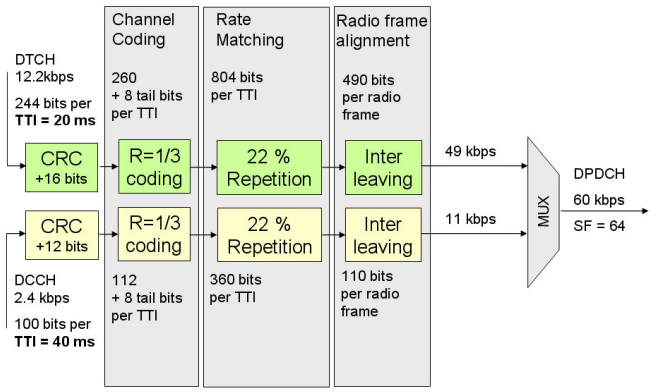

Fig. 3. 12.2 Kbps Uplink Reference channel.

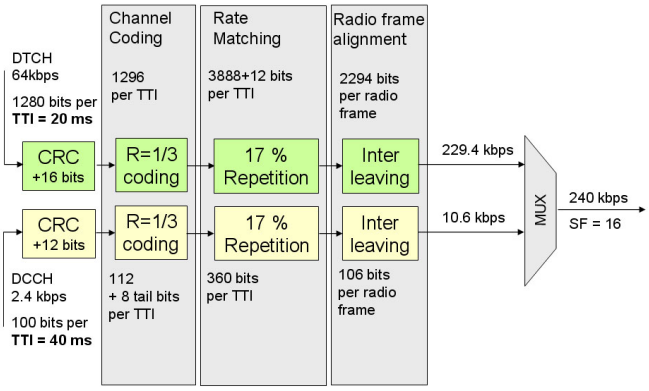

Fig. 4. 64 Kbps Uplink Reference channel.

TABLE II
UPLINK DPDCH DATA RATES.

DPDCH Spreading Factor	DPDCH bit rate	User data rate $\frac{1}{2}$ rate coding
256	15 Kbps	7.5 Kbps
128	30 Kbps	15 Kbps
64	60 Kbps	30 Kbps
32	120 Kbps	60 Kbps
16	240 Kbps	120 Kbps
8	480 Kbps	240 Kbps
4	960 Kbps	480 Kbps
4, with 6 parallel codes	5740 Kbps	2.8 Mbps

of 1.5 meters, is used to determine the coverage region. The path loss coefficient m is 4. The shadow fading standard deviation σ_s is 6 dB. The processing gain $\frac{W}{R_q}$ is 6.02 dB, 12.04 dB, 18.06 dB, and 24.08 dB for Spreading Factor equal to 4, 16, 64, and 256, respectively. The activity factor, v, is 0.375. Fig. 5 shows the 2-D Gaussian approximation of users uniformly distributed in the cells with $\sigma_1 = \sigma_2 = 12000$.

The UMTS network with 27 omnidirectional antenna cells (1 sector per cell) was analyzed for evaluation of capacity using user modeling with the 2-D Gaussian function and traditional methods of modeling uniform user distribution. The network with different values for $\frac{E_b}{I_0}$ was analyzed for different SF values of 4, 16, 64, and 256.

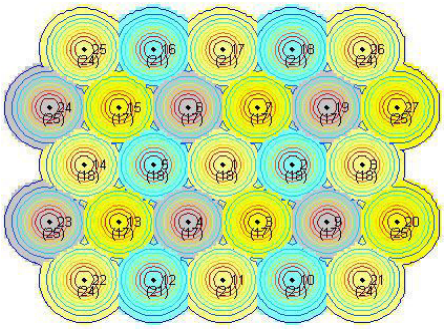

Fig. 5. 2-D Gaussian approximation of users uniformly distributed in the cells. $\sigma_1 = \sigma_2 = 12000$, $\mu_1 = \mu_2 = 0$.

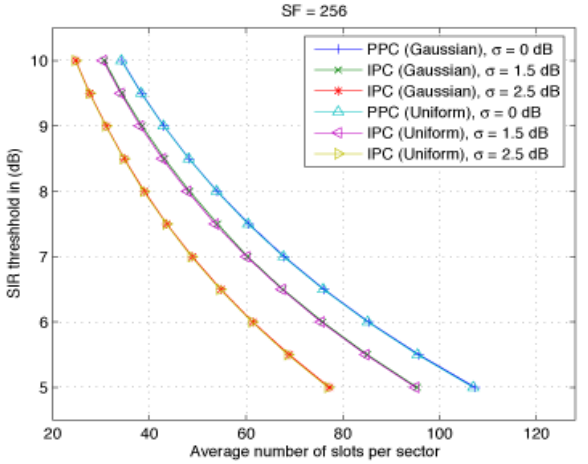

Fig. 6. Average number of slot per sector for perfect and imperfect power control analysis with a Spreading Factor of 256.

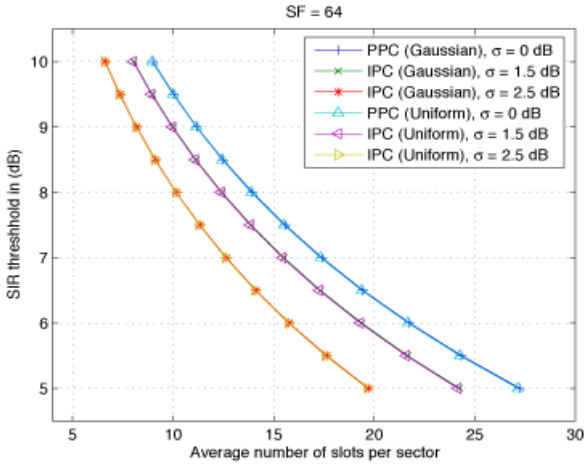

Fig. 7. Average number of slot per sector for perfect and imperfect power control analysis with a Spreading Factor of 64.

A. Capacity Allocation with SF of 256

First, we set SF to 256, which is used to carry data for the control channel. Fig. 6 shows the maximized average number of slots per sector for the 27 cells UMTS network as the $\frac{E_b}{I_0}$ is increased from 5 dB to 10 dB and the standard deviation of imperfect power control is increased from 0 to 2.5 dB. Because of IPC, to get the same average number of slots per sector as PPC, we have to decrease the SIR threshold by 0.5 dB to 1.5 dB. Fig. 6 also shows that the traditional uniform user distribution modeling matches well with the 2-D Gaussian model.

B. Capacity Allocation with SF of 64

As a result of lowering the SF to 64, the number of slots per sector decreases by almost a factor of 4 compared to SF equal 256 (from 60.58 to 15.56 slots when $\frac{E_b}{I_o}$ = 7.5 dB in PPC) as shown in Fig. 7.

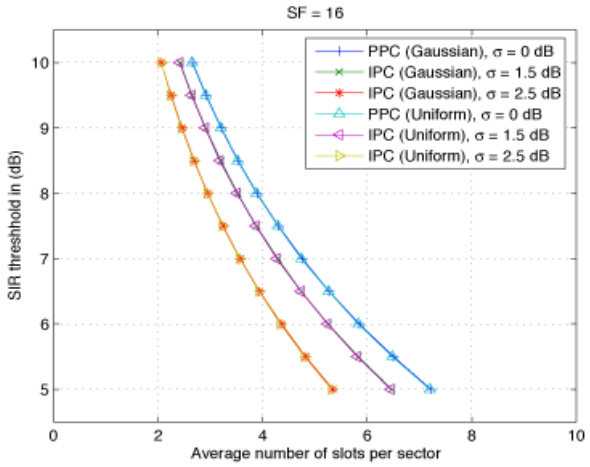

Fig. 8. Average number of slot per sector for perfect and imperfect power control analysis with a Spreading Factor of 16.

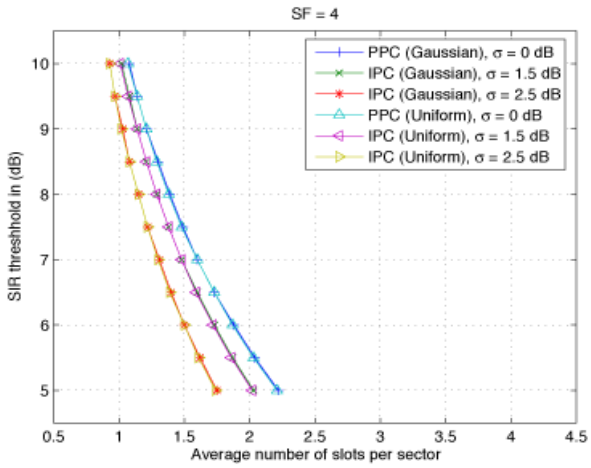

Fig. 9. Average number of slot per sector for perfect and imperfect power control analysis with a Spreading Factor of 4.

C. Capacity Allocation with SF of 16

As a result of lowering the SF to 16, the number of slots per sector decreases by almost a factor of 4 compared to SF equal 64 (from 15.56 to 4.30 slots when $\frac{E_b}{I_o}$ = 7.5 dB in PPC) as shown in Fig. 8.

D. Capacity Allocation with SF of 4

Next, we set SF to 4, which is used for 256 kbps data communication between BSs and MSs. As a result of lowering the SF to 4, the number of slots per sector decreases significantly to 1.49 while keeping $\frac{E_b}{I_o}$ = 7.5 dB in PPC as shown in Fig. 9.

The following set of results are for the calculation of throughput. Three mobility scenarios: no mobility, low mobility, and high mobility of users are considered. We assume that the mobility characteristics for a given service g stays the same throughout different cells in the network. The following parameters are used for the no mobility case: $q_{ij,g}$ = 0, $q_{ii,g}$ = 0.3 and $q_{i,g}$ = 0.7 for all cells i and j. Tables III and IV show respectively the

TABLE III
THE LOW MOBILITY CHARACTERISTICS AND PARAMETERS.

A_i	$q_{ij,g}$	$q_{ii,g}$	$q_{i,g}$
3	0.020	0.240	0.700
4	0.015	0.240	0.700
5	0.012	0.240	0.700
6	0.010	0.240	0.700

TABLE IV
THE HIGH MOBILITY CHARACTERISTICS AND PARAMETERS.

A_i	$q_{ij,g}$	$q_{ii,g}$	$q_{i,g}$
3	0.1	0	0.700
4	0.075	0	0.700
5	0.060	0	0.700
6	0.050	0	0.700

- A_i is the number of cells, which are adjacent to cell i.
- $q_{ii,g}$ is the probability that a call with service g in progress in cell i remains in cell i after completing its dwell time.
- $q_{ij,g}$ is the probability that a call with service g in progress in cell i after completing its dwell time goes to cell j.
- $q_{i,g}$ is the probability that a call with service g in progress in cell i departs from the network.

mobility characteristics and parameters for the low and high mobility cases. In all three mobility scenarios, the probability that a call leaves the network after completing its dwell time is 0.7. Thus, regardless of where the call originates and mobility scenario used, the average dwell time of a call in the network is constant. In the numerical results below, for each SF value, we analyze the average throughput per cell by dividing the results from (23) by the total number of cells in the network and multiplying by the maximum data rate in Table II.

E. Throughput Optimization with SF of 256

First, we set SF equal to 256, which is used to carry data for the control channel. Table V shows the optimized values of **N** for each cell for all three mobility models with perfect power control and 2% blocking probability. Fig. 10 shows the optimized throughput per cell for a blocking probability from 1% to 10%. The results for the average throughput for no mobility and high mobility cases are almost identical while the throughput for low mobility is higher for each blocking probability. The low mobility case has an equalizing effect on traffic resulting in slightly higher throughput.

F. Throughput Optimization with SF of 64

Next, we set SF equal to 64, which is used for voice communication as shown in Fig. 3. As a result of lowering the SF to 64, the number of possible concurrent connections within one cell is also decreased. Because the throughput is calculated based on the number of simultaneous connections between MSs and BSs, the lower trunking efficiency leads to lower throughput as shown in Fig. 11. Table VI shows the optimized values of **N** for each cell for all three mobility cases and SF equal to 64.

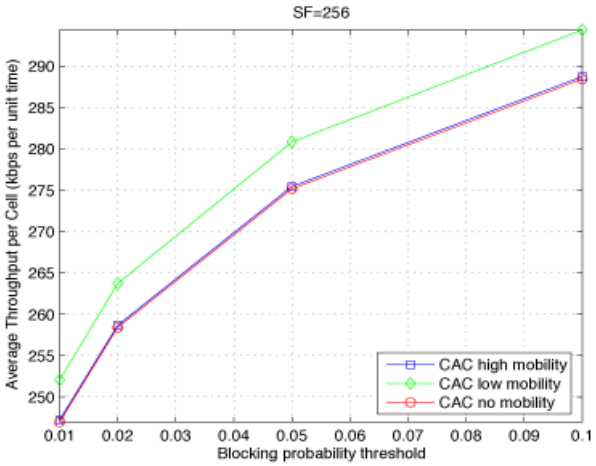

Fig. 10. Average throughput in each cell for SF = 256.

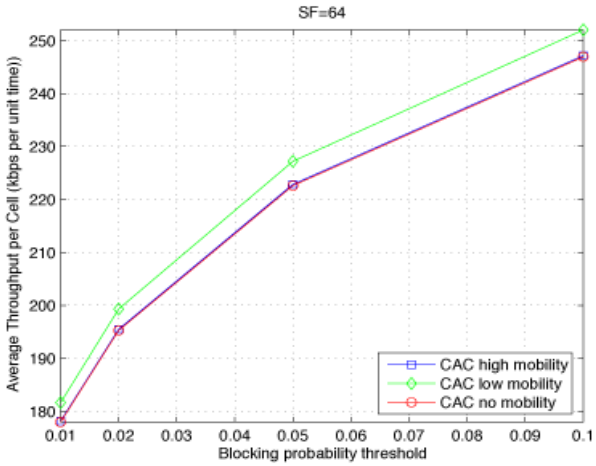

Fig. 11. Average throughput in each cell for SF = 64.

TABLE V
CALCULATION OF **N** FOR UNIFORM USER DISTRIBUTION WITH SF = 256 AND BLOCKING PROBABILITY = 0.02.

	No Mobility	Low Mobility	High Mobility
Cell ID	N_i	N_i	N_i
$Cell_1$	52.86	52.86	52.86
$Cell_2$	53.95	53.95	53.95
$Cell_3$	51.84	51.84	51.84
$Cell_4$	51.84	51.84	51.84
$Cell_5$	53.95	53.95	53.95
$Cell_6$	51.85	51.85	51.85
$Cell_7$	51.85	51.85	51.85
$Cell_8$	53.00	53.00	53.00
$Cell_9$	50.73	50.73	50.73
$Cell_{10}$	62.74	62.74	62.74
$Cell_{11}$	63.29	63.29	63.29
$Cell_{12}$	62.73	62.73	62.73
$Cell_{13}$	50.73	50.73	50.73
$Cell_{14}$	53.01	53.01	53.01
$Cell_{15}$	50.73	50.73	50.73
$Cell_{16}$	62.71	62.71	62.71
$Cell_{17}$	63.27	63.27	63.27
$Cell_{18}$	62.71	62.71	62.71
$Cell_{19}$	50.74	50.74	50.74
$Cell_{20}$	73.40	73.40	73.40
$Cell_{21}$	71.84	71.84	71.84
$Cell_{22}$	71.86	71.86	71.86
$Cell_{23}$	73.43	73.43	73.43
$Cell_{24}$	73.43	73.43	73.43
$Cell_{25}$	71.83	71.83	71.83
$Cell_{26}$	71.82	71.82	71.82
$Cell_{27}$	73.40	73.40	73.40

TABLE VI
CALCULATION OF **N** FOR UNIFORM USER DISTRIBUTION WITH SF = 64 AND BLOCKING PROBABILITY = 0.02.

	No Mobility	Low Mobility	High Mobility
Cell ID	N_i	N_i	N_i
$Cell_1$	13.58	13.58	13.58
$Cell_2$	13.86	13.86	13.86
$Cell_3$	13.32	13.32	13.32
$Cell_4$	13.32	13.32	13.32
$Cell_5$	13.86	13.86	13.86
$Cell_6$	13.32	13.32	13.32
$Cell_7$	13.32	13.32	13.32
$Cell_8$	13.61	13.61	13.61
$Cell_9$	13.03	13.03	13.03
$Cell_{10}$	16.11	16.11	16.11
$Cell_{11}$	16.26	16.26	16.26
$Cell_{12}$	16.11	16.11	16.11
$Cell_{13}$	13.03	13.03	13.03
$Cell_{14}$	13.62	13.62	13.62
$Cell_{15}$	13.03	13.03	13.03
$Cell_{16}$	16.11	16.11	16.11
$Cell_{17}$	16.25	16.25	16.25
$Cell_{18}$	16.11	16.11	16.11
$Cell_{19}$	13.03	13.03	13.03
$Cell_{20}$	18.85	18.85	18.85
$Cell_{21}$	18.45	18.45	18.45
$Cell_{22}$	18.46	18.46	18.46
$Cell_{23}$	18.86	18.86	18.86
$Cell_{24}$	18.86	18.86	18.86
$Cell_{25}$	18.45	18.45	18.45
$Cell_{26}$	18.45	18.45	18.45
$Cell_{27}$	18.85	18.85	18.85

G. Throughput Optimization with SF of 16

Next, we set SF equal to 16, which is used for 64 Kbps data communication as shown in Fig. 4. As a result of lowering the SF to 16, the average number of slots within one cell decreases to 4.30. The resulting throughput, as shown in Fig. 12, is much lower compared to the case with SF equal to 64 or 256. Table VII shows the optimized values of **N** for each cell for all three mobility cases with SF equal to 16.

H. Throughput Optimization with SF of 4

Next, we set SF equal to 4, which is normally used for 256 Kbps data communication between BSs and MSs. As a result of lowering the SF to 4, the average slots per sector decreases significantly to 1.49 with perfect power control and $\frac{E_b}{I_0}$ = 7.5 dB as shown in Fig. 9. Table VII shows the optimized values of **N** for each cell for all three mobility models with SF equal to 4. The average throughput for all three mobility cases are almost identical as shown in Fig. 13.

VIII. CONCLUSIONS

An analytical model has been presented for calculating capacity in multi-cell UMTS networks. Numerical results show that the SIR threshold for the received signals is decreased by 0.5 to 1.5 dB due to the imperfect power control. As expected, we can have many low rate voice users or fewer data users as the data rate increases. The

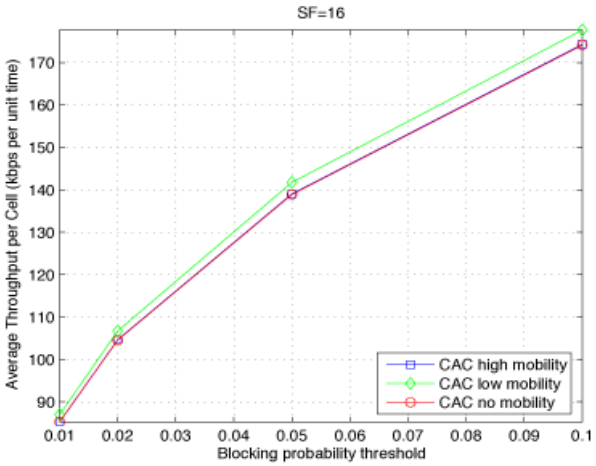

Fig. 12. Average throughput in each cell for SF = 16.

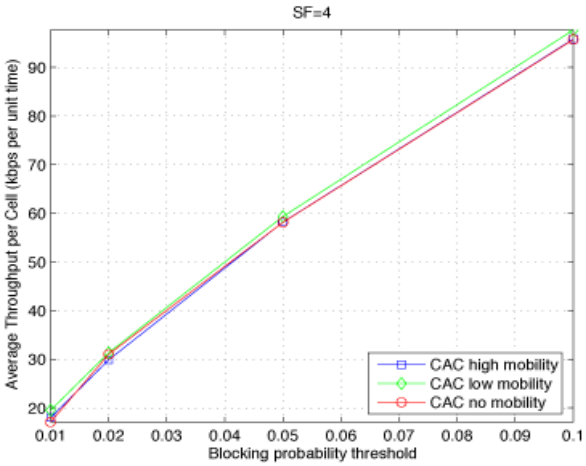

Fig. 13. Average throughput in each cell for SF = 4.

TABLE VII
CALCULATION OF **N** FOR UNIFORM USER DISTRIBUTION WITH SF = 16 AND BLOCKING PROBABILITY = 0.02.

	No Mobility	Low Mobility	High Mobility
Cell ID	N_i	N_i	N_i
$Cell_1$	3.75	3.75	3.75
$Cell_2$	3.83	3.83	3.83
$Cell_3$	3.68	3.68	3.68
$Cell_4$	3.68	3.68	3.68
$Cell_5$	3.83	3.83	3.83
$Cell_6$	3.68	3.68	3.68
$Cell_7$	3.68	3.68	3.68
$Cell_8$	3.76	3.76	3.76
$Cell_9$	3.60	3.60	3.60
$Cell_{10}$	4.46	4.46	4.46
$Cell_{11}$	4.50	4.50	4.50
$Cell_{12}$	4.46	4.46	4.46
$Cell_{13}$	3.60	3.60	3.60
$Cell_{14}$	3.77	3.77	3.77
$Cell_{15}$	3.60	3.60	3.60
$Cell_{16}$	4.45	4.45	4.45
$Cell_{17}$	4.49	4.49	4.49
$Cell_{18}$	4.45	4.45	4.45
$Cell_{19}$	3.60	3.60	3.60
$Cell_{20}$	5.21	5.21	5.21
$Cell_{21}$	5.10	5.10	5.10
$Cell_{22}$	5.10	5.10	5.10
$Cell_{23}$	5.22	5.22	5.22
$Cell_{24}$	5.22	5.22	5.22
$Cell_{25}$	5.10	5.10	5.10
$Cell_{26}$	5.10	5.10	5.10
$Cell_{27}$	5.21	5.21	5.21

TABLE VIII
CALCULATION OF **N** FOR UNIFORM USER DISTRIBUTION WITH SF = 4 AND BLOCKING PROBABILITY = 0.02.

	No Mobility	Low Mobility	High Mobility
Cell ID	N_i	N_i	N_i
$Cell_1$	1.24	1.16	1.32
$Cell_2$	1.48	1.42	1.24
$Cell_3$	1.30	1.32	1.28
$Cell_4$	1.30	1.32	1.28
$Cell_5$	1.48	1.42	1.23
$Cell_6$	1.30	1.32	1.28
$Cell_7$	1.30	1.32	1.28
$Cell_8$	0.94	1.37	1.23
$Cell_9$	0.93	0.94	1.27
$Cell_{10}$	1.59	1.58	1.54
$Cell_{11}$	1.53	1.53	1.55
$Cell_{12}$	1.59	1.58	1.54
$Cell_{13}$	0.93	0.94	1.27
$Cell_{14}$	0.94	1.37	1.23
$Cell_{15}$	0.93	0.93	1.27
$Cell_{16}$	1.59	1.58	1.54
$Cell_{17}$	1.53	1.53	1.55
$Cell_{18}$	1.59	1.58	1.54
$Cell_{19}$	0.93	0.93	1.27
$Cell_{20}$	1.92	1.83	1.82
$Cell_{21}$	1.79	1.80	1.76
$Cell_{22}$	1.79	1.80	1.76
$Cell_{23}$	1.92	1.83	1.82
$Cell_{24}$	1.92	1.83	1.82
$Cell_{25}$	1.79	1.80	1.76
$Cell_{26}$	1.79	1.80	1.76
$Cell_{27}$	1.92	1.83	1.82

results also show that the determined parameters of the 2-dimensional Gaussian model matches well with traditional methods for modeling uniform user distribution. An analytical model was also presented for CAC algorithm for optimizing the throughput in multi-cell UMTS networks. Numerical results show that as the spreading factor increases, the optimized throughput is better, due to the trunking efficiency for all three mobility models (no, low, and high mobility). Our methods for maximizing capacity and implementing the CAC algorithm are fast, accurate, and can be implemented for large multi-cell UMTS networks.

REFERENCES

[1] CDMA Development Group, "CDG : Worldwide : CDMA Worldwide," http://www.cdg.org/worldwide/index.asp?h_area=0.

[2] T. Ojanpera, J. Skold, J. Castro, L. Girard, and A. Klein, "Comparison of multiple access schemes for UMTS," *IEEE Veh. Technol. Conf.*, vol. 2, pp. 490–494, May 1997.

[3] Q. Zhang and O. Yue, "UMTS air interface voice/data capacity-part 1: reverse link analysis," *IEEE Veh. Technol. Conf.*, vol. 4, pp. 2725 – 2729, May 2001.

[4] A. Viterbi, *CDMA Principles of Spread Spectrum Communication*. Addison-Wesley, 1995.

[5] Q. Zhang, "UMTS air interface voice/data capacity-part 2: forward link analysis," *IEEE Veh. Technol. Conf.*, vol. 4, pp. 2730 – 2734, May 2001.

[6] J. Carnero, K. Pedersen, and P. Mogensen, "Capacity gain of an uplink-synchronous WCDMA system under channelization code constraints," *IEEE Veh. Technol. Conf.*, vol. 53, pp. 982 – 991, July 2004.

[7] R. Akl, M. Hegde, M. Naraghi-Pour, and P. Min, "Multi-cell CDMA network design," *IEEE Trans. Veh. Technol.*, vol. 50, no. 3, pp. 711–722, May 2001.

[8] S. Nguyen and R. Akl, "Approximating user distributions in WCDMA networks using 2-D Gaussian," *Proceedings of International Conf. on Comput., Commun., and Control Technol.*, July 2005.

[9] D. Staehle, K. Leibnitz, K. Heck, B. Schroder, A. Weller, and P. Tran-Gia, "Approximating the othercell interference distribution in inhomogenous UMTS networks," *IEEE Veh. Technol. Conf.*, vol. 4, pp. 1640–1644, May 2002.

[10] T. Tugcu and C. Ersoy, "Application of a realistic mobility model to call admissions in DS-CDMA cellular systems," *IEEE Veh. Technol. Conf.*, vol. 2, pp. 1047–1051, Spring 2001.

[11] P. Orlik and S. Rappaport, "On the handoff arrival process in cellular communications," *Wireless Networks*, vol. 7, pp. 147–157, 2001.

[12] Y. Fang, I. Chlamtac, and Y.-B. Lin, "Modeling PCS networks under general call holding time and cell residence time distributions," *IEEE/ACM Trans. on Networking*, vol. 5, pp. 893–906, 1997.

[13] C. Vargas, M. Hegde, and M. Naraghi-Pour, "Implied costs for multi-rate wireless networks," *J.Wireless Networks*, vol. 10, pp. 323–337, May 2004.

[14] V. Istratescu, *Fixed Point Theory : An Introduction*. D. Reidel, 1981.

[15] R. Akl, M. Hegde, and P. Min, "Effects of call arrival rate and mobility on network throughput in multi-cell CDMA," *IEEE International Conf. on Commun.*, vol. 3, pp. 1763–1767, June 1999.

[16] F. Kelly, "Routing in circuit-switched network: Optimization, shadow prices and decentralization," *Advances in Applied Probability*, vol. 20, pp. 112–144, 1988.

[17] D. Mitra, J. Morrison, and K. Ramakrishnan, "ATM network design and optimization: a multirate loss network framework," *IEEE/ACM Trans. on Networking*, vol. 4, no. 4, pp. 531–543, August 1996.

[18] C. Vargas, M. Hegde, and M. Naraghi-Pour, "Blocking effects of mobility and reservations in wireless networks," *IEEE International Conf. on Commun.*, vol. 3, pp. 1612–1616, June 1998.

[19] ——, "Implied costs in wireless networks," *IEEE Veh. Technol. Conf.*, vol. 2, pp. 904–908, May 1998.

[20] C. Vargas-Rosales, "Communication network design and evaluation using shadow prices," Ph.D. dissertation, Louisiana State University, 1996.

[21] F. Kelly, "Blocking probabilities in large circuit switched networks," *Advances in Applied Probability*, vol. 18, pp. 473–505, 1986.

[22] A. F., S. M., and O. K., "Tree-structured generation of orthogonal spreading codes with different lengths for forward link of DS-CDMA mobile radio," *Electr. Lett.*, vol. 33, pp. 27–28, January 1997.

[23] R. Akl and A. Parvez, "Impact of interference model on capacity in CDMA cellular networks," *Proceedings of SCI 04: Communication and Network Systems, Technologies and Applications*, vol. 3, pp. 404–408, July 2004.

[24] R. Akl, M. Hegde, and M. Naraghi-Pour, "Mobility-based CAC algorithm for arbitrary traffic distribution in CDMA cellular systems," *IEEE Trans. Veh. Technol.*, vol. 54, pp. 639–651, March 2005.

Robert Akl received the B.S. degree in computer science from Washington University in St. Louis, in 1994, and the B.S., M.S. and D.Sc. degrees in electrical engineering in 1994, 1996, and 2000, respectively. He also received the Dual Degree Engineering Outstanding Senior Award from Washington University in 1993. He is a senior member of IEEE.

Dr. Akl is currently an Assistant Professor at the University of North Texas, Department of Computer Science and Engineering. In 2002, he was an Assistant Professor at the University of New Orleans, Department of Electrical and Computer Engineering. From October 2000 to December 2001, he was a senior systems engineer at Comspace Corporation, Coppell, TX. His research interests include wireless communication and network design and optimization.

Son Nguyen received the B.S. degree in computer science and the M.S. degree in computer science from The University of North Texas in 2001 and 2005, respectively. His research interests include 3G wireless network design and optimization.